Depth profile investigations of silicon nanocrystals formed in sapphire by ion implantation

S. Yerci,[a] I Yildiz, and M. Kulakci
Department of Physics, Middle East Technical University, 06531 Ankara, Turkey

U. Serincan
Department of Physics, Middle East Technical University, 06531 Ankara, Turkey, and Department of Physics, Anadolu University, Eskisehir, 26470, Turkey

M. Barozzi and M. Bersani
ITC-Irst, Via Sommarive 18, 38050 Povo-Trento, Italy

R. Turan
Department of Physics, Middle East Technical University, 06531 Ankara, Turkey

(Received 27 March 2007; accepted 6 June 2007; published online 24 July 2007)

Depth profiles of Si nanocrystals formed in sapphire by ion implantation and the effect of charging during X-ray Photoelectron Spectroscopy (XPS) and Secondary Ion Mass Spectrometry (SIMS) measurements have been studied. Atomic concentration and the chemical environment of Si, Al, and O have been measured as a function of depth from the sample surface by SIMS and XPS. Both as-implanted and annealed samples have been analyzed to understand the effect of nanocrystal formation on the depth distribution, chemical structure, and the charging effect before and after the formation process. SIMS measurements have revealed that the peak position of the Si concentration shifts to deeper values with implantation dose. This is explained by the fact that the structure of the matrix undergoes a phase transformation from pure sapphire to a Si rich amorphous Al_2O_3 with heavy dose implantation. Formation of Si nanocrystals has been observed by XPS by an increase in the Si-Si signal and a decrease in Si-O bond concentrations after the annealing. Variation in binding energies of Si and O with Si concentration (i.e., with depth) has been studied in terms of chemical environments and charging effects. It is found that binding energy of these elements shifts to lower values with increasing Si content. This is a result of less charging due to the presence of easy discharge paths in the Si rich regions of the matrix. Nanocrystal formation leads to even less charging which is probably due to the further increase in conductivity with the formation. © *2007 American Institute of Physics*. [DOI: 10.1063/1.2756622]

I. INTRODUCTION

Si nanocrystals (Si-ncs) embedded in oxides have been an extensive research topic due to their superior and future promising applications in nonvolatile memory and light emitting devices.[1–3] Replacement of poly-Si or metal floating gate in metal-oxide-semiconductor (MOS) structures with densely packed arrays of Si-ncs is believed to lead the next generation memory devices operating at low powers and having high retention times.[3,4] It is known that a leakage current between the floating gate and substrate in MOS structures can empty the electrons in the gate and therefore destroy stored information. Use of nanocrystals as the storage medium in the gate is expected to improve the reliability by distributing the total stored charge in discrete quantum dots isolated from each other.[3] An electrical short between one individual nanocrystal and the substrate will not affect the charges stored in the rest of the device. Prototypes of Si-ncs based MOS structures have already been demonstrated using SiO_2, Al_2O_3, and HfO_2 as tunneling oxides.[4–7] SiO_2 is universally used due to its compatibility with existing Si technology.[7] However, high-k materials such as Al_2O_3 and HfO_2 having dielectric constants higher than SiO_2 (Refs. 4–6) are expected to improve the reliability and hence decrease the device dimensions. Capacitance-voltage measurements are widely employed to characterize the charging/discharging mechanisms in these devices.[4–7] In addition, charging in and on the Si-ncs embedded in the SiO_2 matrix has recently been studied from a different perspective by using x-ray photoelectron spectroscopy (XPS).[8–14] Dane *et al.* have reported effect of charging in Si-ncs produced by plasma enhanced chemical vapor deposition using XPS with external voltage stimuli and time resolved techniques while Chen *et al.* have dealt with the same structure produced by ion implantation technique by correcting the spectrum according to C 1*s* signal of surface contamination.[8,9] Both groups found a ~0.6 eV shift to lower binding energies for Si^0 signal of nanocrystals according to the signal of bulk Si. Although they attributed this shift to the differential charging between the Si-ncs and SiO_2 host matrix they were not able to detect a differential character of charging.

XPS is a powerful technique in the sense that the atomic composition and chemical state of the elements can be probed with a fairly good accuracy. Therefore, it can be used to show the phase separation of nanoclusters, i.e., transition

[a]Present address: Department of Electrical and Computer Engineering, Boston University, Boston, MA 02215; electronic mail: syerci@bu.edu

of the matrix from SiO_x ($x<2$) to SiO_2 with Si nanoclusters during the heat treatment.[10] It is known that bulk Si and SiO_2 have binding energies of 99.3 and 103.4 eV, respectively. Binding energies of Si suboxides, Si_2O, SiO, Si_2O_3 are between these two values with nearly 1 eV shift between each state.[10] However, charging in insulator can also create a shift in the spectrum which makes the analysis complicated.[11] Although several methods were developed to overcome the charging problem it is not possible to eliminate this effect completely.[11] The most commonly used correction method is based on the assumption that peak position of the C 1*s* signal arising from the surface contamination is located at 285 eV and any shift from this value should directly be related to the charging. All other peaks are then corrected by using this charging induced shift value. In spite of uncertainties of the assumptions used, this approach has also been adapted to the analysis of charging in Si-ncs.[9–11] Moreover, this method cannot be used during the depth measurements due to absence of carboxyl layer underneath the surface in many cases. Depth profile of the elements and their chemical environments can be monitored in XPS by measuring after successive sputtering. In this case, accelerated ions can cause knock-on implantation, atomic intermixing, preferential etching, and bond breaking, which make the analysis more complicated.[12]

In this study, silicon nanocrystals were formed in α-Al_2O_3 matrix by ion implantation and subsequent annealing process. Depth profiles of the Si, O, and Al atoms of the as-implanted samples were monitored using XPS and secondary ion mass spectrometry (SIMS). XPS was also used to investigate the phase separation and to show the nanocrystal formation by monitoring intensity variations of the oxidation states of Si. Shift in the spectra of *as*-implanted and the annealed samples was compared and studied to understand possible charging/discharging mechanisms.

II. EXPERIMENTAL

C-plane oriented α-Al_2O_3 substrates were implanted with 100 keV $^{28}Si^+$ ions at novel doses of 2×10^{16}, 1×10^{17}, and 2×10^{17} Si/cm^2. The implanted samples annealed at temperatures between 600–1200 °C in N_2 ambient for 2 h to form Si-ncs. SIMS depth profile was obtained with Cameca (4-f) SC-Ultra instrument. A Cs^+ primary beam with an impact energy of 3 keV was used. The $^{133}Cs^{28}Si^+$, $^{133}Cs^{16}O^+$, and $^{133}Cs^{27}Al^+$ secondary ion species were monitored in order to reduce the matrix effects.[15] Samples were initially coated with Au to decrease the charging effect during the sputtering process. SIMS measurements were terminated when the $^{133}Cs^{28}Si^+$ signal reached its maximum value. The depth of the SIMS craters was measured with a mechanical profilometer to find the projected range of the implanted ions. XPS measurements were done with a Specs XPS system at a vacuum of 1×10^{-7} Pa equipped with a hemispherical electron analyzer operated with a focusing lens at a spot size of 750 μm and at a take-off angle of 90°. Mg $K\alpha$ line with a power of 200 W was used as the excitation source. Depth profiles of Si, O, and Al atoms were recorded by sputtering the sample surface with Ar^+ ions with an energy of 4000 eV and an angle of 40° with cycles of 5 and 8 min for the as-implanted and annealed samples, respectively. An area of 3×3 mm^2 was etched out and the ejected electrons were collected from the center of the sample to avoid the edge effect. XPS measurements were performed with a step size of 0.1 eV and pass energy of 96 eV. Data analysis techniques (background correction and peak fit) were applied to improve the data evaluation using XPSPEAK95 software.[16] Raman measurements were employed in backscattering geometry at room temperature using 632.8 nm as a light source of a confocal micro-Raman (HR800, Jobin Yvon), attached with Olympus microanalysis system and a CCD camera providing a resolution of ~1 cm^{-1}.

III. RESULTS AND DISCUSSION

A. Secondary ion mass spectrometry (SIMS)

The projected range of implantation, i.e., peak position of Si ion distribution in the matrix, was calculated as ~81.5 nm using TRIM simulation which assumes uniform and unchanged matrix during the implantation process.[17] However, actual projected ranges were measured as ~119.0, 125.1, and 131.2 nm for samples with nominal doses of 2×10^{16}, 1×10^{17}, and 2×10^{17} Si/cm^2 using SIMS. These values are significantly greater than what is estimated by TRIM simulation. The calculated and measured depth profiles of Si ions are given in Fig. 1. It is clearly seen that both peak concentration and peak position of Si ions as measured with SIMS increase with the implantation dose. We previously reported a similar phenomenon for sapphire samples implanted with Ge ions using transmission electron microscopy (TEM).[18,19] It is known that ions can penetrate deeper in the crystalline matrix by the channeling effect. Since the sapphire substrate is amorphized during high dose implantation and the channeling effect is expected to be reduced after the implantation, the observed increase in the projected range with the dose of the implantation cannot be attributed to the channeling effect. Instead, the variation of the projected range with the dose should be related to the modification of the chemical content of the sapphire matrix. In order to understand the effect of such a modification on the Si depth distribution, we run the TRIM simulation by assuming the presence of a 20 nm thick Si layer between 70–90 nm underneath the surface. This represents a reasonable approximation to the actual case. The projected range was calculated as 109.4 nm which is closer to the value measured by SIMS. This simple calculation shows qualitatively that the projected range increases with inclusion of Si atoms into the matrix. The agreement between this value and the measured one can further be improved with a more dynamic simulation incorporating the chemical and structural variations of the matrix into the calculation.

The change of the total mean sputtering rates for the as-implanted sample and samples annealed at 700, 900, 1050, and 1200 °C are given in the inset of Fig. 1. These mean rates were determined by measuring the depth of the crater after the measurement and time for the SIMS analysis. We see that the sputter rate approaches that of virgin sap-

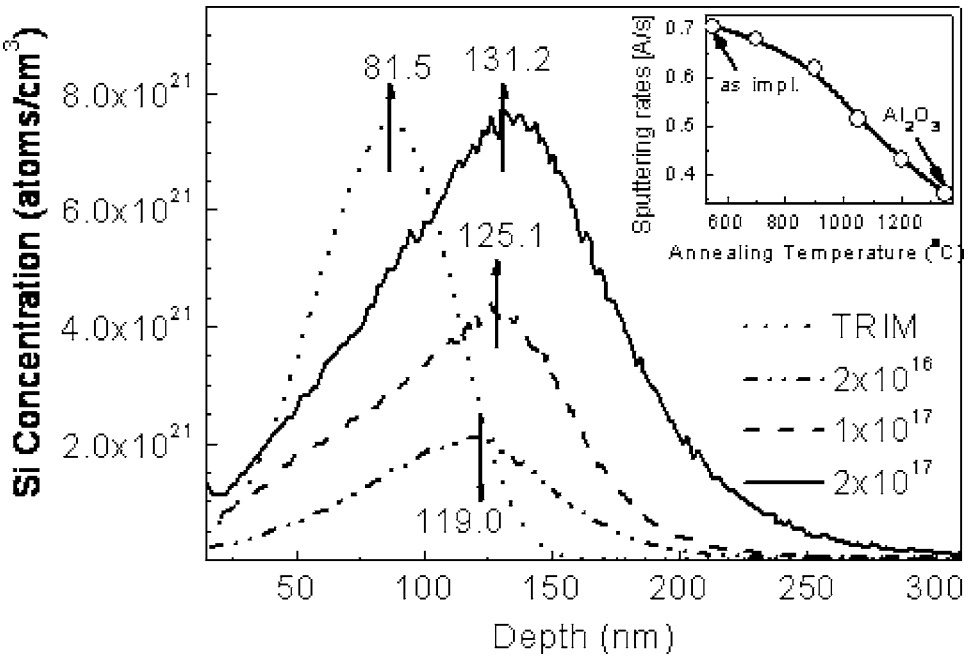

FIG. 1. Depth profiles of Si ions using SIMS for samples implanted with nominal doses of 2×10^{16}, 1×10^{17}, and 2×10^{17} Si/cm^2. Depth profile calculated by TRIM simulation is also shown. The change of the total mean sputtering rates for the as-implanted sample and samples annealed at 700, 900, 1050, and 1200 °C are given in the inset.

phire as the temperature of annealing increases, indicating the recovery of the matrix at higher temperatures.

It should also be noted that phase separation of the Si-ncs formed into SiO_2 was previously studied using time of flight SIMS by monitoring the signals of the $Si_n^-(1\leq n<6)$ species.[20] However, in the present work, $Si_n^+(n>2)$ species could not be detected by SIMS due to their low intensity and charging of the matrix.

B. X-ray photoelectron spectroscopy (XPS)

1. Si depth profile and the diffusion of Si atoms

XPS depth profile of Si 2*p* signals of the as-implanted and annealed samples are given in Fig. 2. The XPS and SIMS profiles of the as-implanted sample are in consistence with each other. The highest relative concentration of Si atoms is measured as 15% using XPS at the projection range of implantation. On the other hand, as it is seen from Fig. 2(a), there is no Si near the surface region of the as-implanted sample (within the detection limits of XPS) as expected from both TRIM simulation and SIMS measurements. However, unlike the as-implanted sample, Si 2*p* signals were observed even at the surface of the film indicating the out diffusion of Si atoms toward the surface of the annealed sample as shown in Fig. 2(b). Similarly, the out diffusion of Ge atoms in Al_2O_3 structure was previously observed using Rutherford backscattering.[21] This redistribution is likely to result from trapping effects of the surface which act as a sink for the atoms moving to the surface.[22]

2. Phase separation of Si atoms and nanocrystal formation

The Si 2*p* signal is a combination of five oxidation states of Si^{n+} (n=0, 1, 2, 3, and 4) corresponding to the chemical structures of Si, Si_2O, SiO, Si_2O_3, and SiO_2, respectively.[10,19] Deconvolution of Si 2*p* signals for the as-implanted sample and the sample annealed at 1000 °C are given in Fig. 3. Both signals were measured where the Si 2*p* signals are highest. The higher peak shown in Fig. 3(a) around 101 eV is due to the Si^0 signal while the shoulder at the higher binding energy side is due to the oxidation states. From Figs. 3(a) and 3(b), phase separation of Si atoms and disappearance of the Si^{4+} states during the annealing are clearly seen. The binding energy difference between Si^0 and Si^{4+} is around 4.7 eV. Similar values were observed for the thin oxides grown on Si and Si-ncs grown in SiO_2.[8,11,23] According to the Raman signals given in the insets of Figs. 3(a) and 3(b), the Si rich layer formed by ion implantation initially contains amorphous Si which becomes nanocrystalline with annealing.[24] Further-

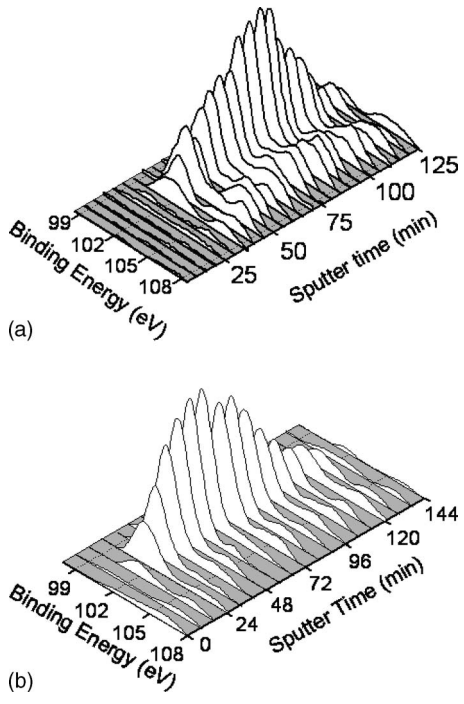

FIG. 2. XPS depth profiles of Si 2*p* signals of the (a) as implanted sample and (b) the sample annealed at 1000 °C.

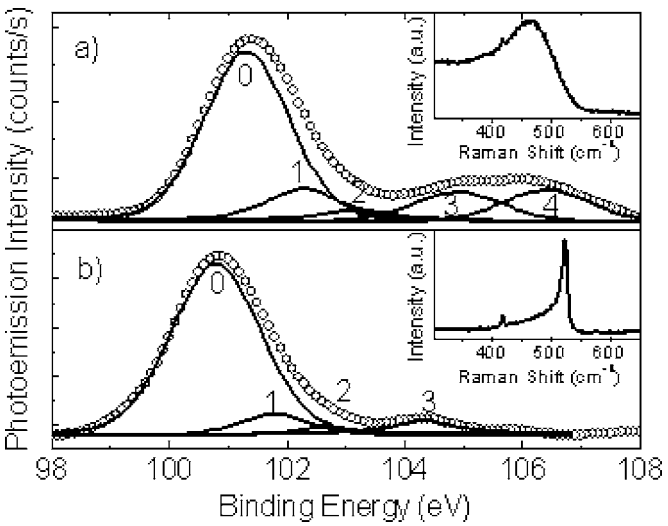

FIG. 3. Deconvolution of Si 2*p* signals of (a) as-implanted sample and (b) samples annealed at 1000 °C. Raman spectra of the as-implanted sample and the sample annealed at 1000 °C are given in the insets of (a) and (b), respectively.

more, using XRD signals, we previously showed that Si-ncs with a mean size of 7.2 nm were formed in the annealed sample.[24]

3. Charging/discharging mechanism in Si nanocrystals

XPS depth profile of O 1*s* signals of the as-implanted and annealed samples are given in Fig. 4. As it is presented in Fig. 4(a), the O 1*s* peak shifts to higher binding energies just under the surface and to lower binding energies with increasing Si concentration as seen in Fig. 5. Two mechanisms can mainly be responsible for the shift in the spectrum: change in the chemical environment and charging/discharging effects.[11] The initial shift to higher binding energies is obviously due to the change in the chemical environment by the removal of adsorbed surface layer (mainly contamination) during the sputtering. The following shift to lower binding energies can be related with both the chemical environment due to the variation of the Si concentration with depth and the charging/discharging of the matrix and nanocrystals.

The peak position of O 1*s* for amorphous SiO_2 is assumed to be around 532.5 eV while that for α-Al_2O_3 is 531.4 eV when C 1*s* peak position is at 285 eV.[25,26] The peak position of O 1*s* peak for Al_2O_3 depends on the phase of the transition crystals but it is expected to be lower than that for SiO_2.[25,26] As the Si-O bond concentration increases toward the projected range the binding energy of the O 1*s* electrons is expected to shift to higher values with depth. This is contrary to what we have observed. Moreover, we did not observe any relative shift between the O 1*s* and Al 2*p* peaks as can be seen from Fig. 5. If the chemical environment was the major cause of the peak shift we should have seen different behavior for these two cases because Al atoms form bonds only with O (Al-O), while O can form both Al and Si bonds (Al-O and Si-O).[23] Increasing Si content in the matrix should not alter the chemical status of Al while it should cause additional variation in the O 1*s* peak. As a result, the observed shift in the XPS peak with depth cannot be attributed to the chemical status of the elements. It should be related to the variation in charging nanocrystals and/or surrounding matrix. Charging is altered by the conductivity variations due to the formation of a Si rich layer (with 15% atomic percentage) buried at around projected range. As the conductivity is expected to increase with increasing Si content in the Al_2O_3 matrix the one could expect less charging in the matrix. This is in agreement with the observed shift in the peak position with depth.[10]

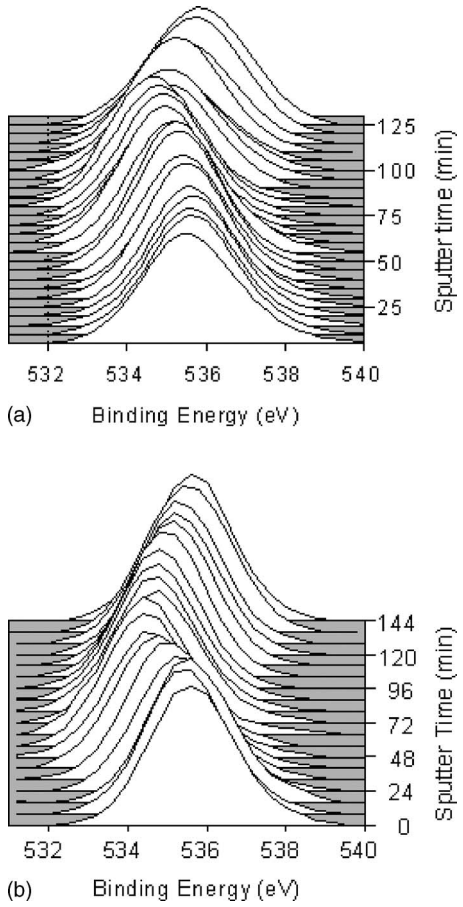

FIG. 4. XPS depth profiles of O 1*s* signals of the (a) as implanted sample and (b) the sample annealed at 1000 °C.

The variation of O 1*s* XPS signal after annealing at 1000 °C is given in Fig. 4(b). Similar to the as-implanted sample, a shift to lower binding energy was observed in the O 1*s* signal with increasing Si concentration [Fig. 4(b)].

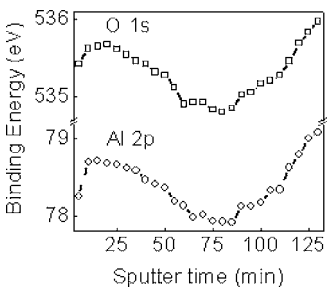

FIG. 5. Shift in the peak positions of O 1*s* and Al 2*p* XPS signals as a function of depth.

However, the magnitude of the shift is higher than that of the as-implanted sample. Contrary to the as-implanted sample, the Si^{4+} signal almost disappeared, showing that the amount of Si-O bonds is significantly reduced with annealing. This is obviously a direct consequence of nanocrystal formation as was clearly demonstrated by many studies.[8–13] The weak Si-O signal remained even after the annealing process is related to SiO_x $(x<2)$ bonds formed at the interface of the nanocrystals. The enhancement in the peak shift with annealing can be due to the decrease in the Si-O bond concentration with the formation of Si-Si bonds (i.e., Si-ncs) or increase in the conductivity of the layer with the nanocrystal formation. An increase in the conductivity leads to the formation of easy escape paths for the trapped charges responsible for the charging effects. This is in agreement with what was reported by Liu *et al.* in a recent paper where they measured the depth profile of Si-ncs formed in SiO_2 by low energy ion implantation.[10] Although they did not consider the charging effect in the as-implanted sample, they explained the lack of charging in the annealed sample near to the projected range with discharging of the surface through the nanocrystals. However, contrary to their report, a complete discharging was not observed in the present study. The peak position of O 1*s* signals is at 534.4 eV at the projected range which is about 2 eV higher than the value that is expected when there is no charging. The lower density of nanocrystals in our sample and higher dielectric constant of Al_2O_3 can decrease the charge diffusion and therefore be responsible for lack of a complete discharging. On the other hand, it should be noted that formation of nanocrystals did not alter the relative positions of Al 2*p* and O 1*s* signals as in the as-implanted sample. As discussed above, this is an additional evidence indicating that the charging/discharging is the main mechanism that determines the shift in the XPS peak position.

IV. CONCLUSIONS

We have reported a SIMS and XPS study on depth distribution, chemical environment, and charging effects of Si-ncs formed in sapphire matrix by ion implantation. We have shown that TRIM calculation of Si atom distribution does not coincide with the measured SIMS profile. This discrepancy is due to the ion beam induced transformation of the matrix during heavy dose implantation. A more dynamic simulation code incorporating variation in the structure of the matrix during the implantation should be used in these cases. The variation of the electron binding energy in Si and Al has been measured as a function of depth by XPS. The nanocrystal formation has manifested itself as an increase in the Si-Si signals and decrease in the Si-O signals. The shift caused by the charging effect is modified by variations in the charging/discharging mechanisms. Presence of excess Si in the Al_2O_3 matrix increases conductivity of the matrix and causes a shift to the lower binding energies. The shift is largest in regions where Si concentration is the highest. It is shown that the shift in the binding energy is enhanced by the formation of nanocrystals due to further increase in the conductivity.

ACKNOWLEDGMENTS

This work has been partially supported by the EU FP6 projects SEMINANO under contract No. NMP4 CT2004 505285 and METU-CENTER with contract No. 17125. The authors would like to thank to Dr. D. Giubertoni for his helpful discussion on SIMS measurements and the METU Central Laboratory for XPS measurements.

[1] K. D. Hirschman, L. Tsybeskov, S. P. Duttagupta, and P. M. Fauchet, Nature **384**, 338 (1996).
[2] L. Pavesi, Z. Gaburro, L. Dal Negro, P. Bettotti, G. Vijaya Prakash, M. Cazzanelli, and C. J. Oton, Opt. Lasers Eng. **39**, 345 (2003).
[3] S. Tiwari, F. Rana, and K. Chan, Appl. Phys. Lett. **68**, 1377 (1996).
[4] A. Dana, I. Akca, A. Aydinli, R. Turan, and T. Finstad, J. Nanosci. Nanotechnol. (to be published).
[5] Y. Zhu, H. Wang, and P. P. Ong, J. Phys. D **33**, 2687 (2000).
[6] P. Punchaipetch, Y. Uraoka, T. Fuyuki, A. Tomyo, E. Takahashi, T. Hayashi, A. Sano, and S. Horii, Appl. Phys. Lett. **89**, 093502 (2006).
[7] W. Skorupa, L. Rebohle, and T. Gebel, Appl. Phys. A **76**, 1049 (2003).
[8] A. Dane, U. K. Demirok, A. Aydinli, and S. Suzer, J. Phys. Chem. B **110**, 1137 (2006).
[9] T. P. Chen, Y. Liu, C. Q. Sun, M. S. Tse, J. H. Hsieh, Y. Q. Fu, Y. C. Liu, and S. Fung, J. Phys. Chem. B **108**, 16609 (2004).
[10] Y. Liu, T. P. Chen, C. Y. Ng, L. Ding, S. Zhang, Y. Q. Fu, and S. Fung, J. Phys. Chem. B **110**, 16499 (2006).
[11] S. Iwata and A. Ishizaka, J. Appl. Phys. **79**, 6653 (1996).
[12] S. Oswald and R. Reiche, Appl. Surf. Sci. **179**, 307 (2001).
[13] D.-Q. Yang, J.-N. Gillet, M. Meunier, and E. Sacher, J. Appl. Phys. **97**, 024303 (2005).
[14] V. Mulloni, P. Bellutti, and L. Vanzetti, Surf. Sci. **585**, 137 (2005).
[15] M. R. Frost and C. W. Magee, Appl. Surf. Sci. **104–105**, 379 (1996).
[16] R. W. M. Kwok, www.phy.cuhk.edu.hk/~surface/XPSPEAK.
[17] J. F. Ziegler, J. P. Biersack, and U. Littmark, *The Stopping and Range of Ions in Solids* (Pergamon, NewYork, 1985).
[18] S. Yerci, M. Kulakci, U.Serincan, M. Shandalov, Y. Golan, and R. Turan, J. Nanosci. Nanotechnol. (to be published).
[19] S. Yerci, I. Yildiz, A. Seyhan, M. Kulakci, U. Serincan, M. Shandalov, Y. Golan, and R. Turan, Mater. Res. Soc. Symp. Proc. **958**, L07–06 (2006).
[20] M. Perego, S. Ferrari, M. Fancuilli, G. Ben Assayag, C. Bonafos, M. Carrada, and A. Claverie, Appl. Surf. Sci. **231–232**, 813 (2004).
[21] I. D. Sharp, Q. Xu, D. O. Yi, C. W. Yuan, J. W. Beeman, K. M. Yu, J. W. Ager III, D. C. Chrzan, and E. E. Haller, J. Appl. Phys. **100**, 114317 (2006).
[22] R. Turan and T. G. Finstad, Philos. Mag. A **63**, 519 (1991).
[23] N. Koshizaki, H. Umehara, and T. Oyama, Thin Solid Films **325**, 130 (1998).
[24] S. Yerci, U. Serincan, I. Dogan, M. S. Tokay, M. F. Genisel, A. Aydinli, and R. Turan, J. Appl. Phys. **100**, 074301 (2006).
[25] V. La Parola, G. Deganello, S. Scire, and A. M. Venezia, J. Solid State Chem. **174**, 482 (2003).
[26] C. Wagner, W. Riggs, L. Davis, and J. Moulder, in *Handbook of X-Ray Photoelectron Spectroscopy*, edited by G. E. Muilenberg (Perkin Elmer Corporation, Eden Prairie, MN, 1979), Vol. 1, pp. 52–53.